PROBABILISTIC PARAMETERS OF THE SEISMIC PERFORMANCE OF REINFORCED CONCRETE FRAMES

Fabio Biondini, Giandomenico Toniolo
Department of Structural Engineering, Technical University of Milan

ABSTRACT

The paper gives a contribution to the reliability assessment of the design methods of Eurocode 8 for concrete structures in seismic zones, with reference to r.c. frame systems. To this purpose a large number of dynamic analyses have been done assuming as many artificial accelerograms. The choice of these accelerograms follows the criteria of the quoted Eurocode, saving the random variability of the main features of real earthquakes, so to apply a Monte Carlo process of probabilistic investigation of structural performance.

The computed responses have been quantified on the base of the overstrength behaviour parameter, for which a statistical evaluation has been done. Some additional considerations are presented about the suitability of the analytical model used in computations, about the representativeness of the random set of ground motion simulations and about the design provisions of Eurocode 8.

In particular the comparison of the responses coming from different arrangement of joint connections (rigid or hinged) shows that the dissipation of energy is not a question of number of dissipation zones, but it is a question of total structural volume involved in dissipation: few larger zones may dissipate the same amount of energy of many smaller zones. This deny the discriminations set by the first version 1994 of Eurocode 8 to some type of one storey precast structures.

Keywords: seismic response, design reliability, concrete structures, simulated earthquakes.

1. INTRODUCTION

Overall models of cyclic degrading stiffness for r.c. members can be easily used for quick dynamic analyses under seismic actions. In some previous works Takeda model has been assumed to simulate cyclic and pseudodynamic tests (Saisi and Toniolo, 1997), reaching a good calibration of its parameters by comparison with the experimental results. Improved with a final falling branch to simulate failure, this model has been subsequently used for an incremental analysis of r.c. structures up to ultimate collapse conditions (Biondini and Toniolo, 2000).

This paper assumes a very simple type of structure so to focus the attention on the overstrength parameter, assumed as representative of the structural behaviour at ultimate conditions.

Seismic action is simulated by artificial accelerograms, which are generated automatically following an envelope curve. The shape of this curve is chosen in such a way so to suite the features of real earthquakes. The artificial signal remains much richer of frequencies than the recorded signal of real earthquakes. All generated accelerograms match the response spectrum of soil type A of Eurocode 8 (version May 2001).

The use of hundreds of artificial accelerograms for a statistical evaluation of the structural response could be improper, since their random variability doesn't save all the larger variabilities of real earthquakes. Nevertheless, these latters cannot supply an homogeneous set, large enough to give a complete statistical representation of any possible future event (Biondini and Toniolo, 2001).

The structure, in its two arrangements corresponding to a cast-in-situ monolithic solution and a precast hinged solution, is described in Fig. 1 (see also Appendix). It is assumed that, under the same seismic force F, the arrangement of Fig. 1.a, with four critical sections dimensioned for a moment $m=Fh/2$, may dissipate the same amount of energy which the arrangement of Fig. 1.b dissipates in its two critical sections, dimensioned as they are for a moment $M=Fh$ double than the first one ($4u \cong 2U$). Thus, both the structures are intended to belong to the "prized" type of frames, with the same force reduction factor. The confirmation of this assumption and the actual quantification of the reduction factor (the behaviour factor of Eurocode 8 - EC8) should come from the results of the analysis.

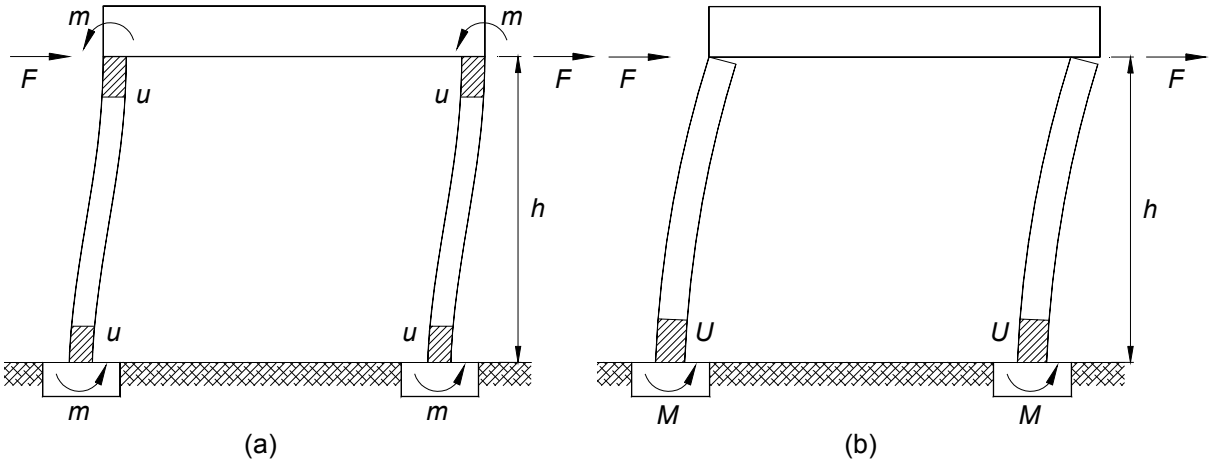

Figure 1. Energy dissipated by the frames: (a) monolithic and (b) hinged arrangement.

The investigation presented in this paper gives only a partial evaluation, which can be referred only to the particular type of structure examined in the analysis, but it represents anyway a step in the direction of a more precise measure of safety reliability, when made on the base of EC8 rules.

2. CHOICE OF THE ACCELEROGRAMS

Eurocode 8, in the prEN Draft May 2001, gives some requirements for artificial accelerograms like the minimum duration of 10 sec of the stationary part. But this requirement refers to a quite different use, since the minimum number of accelerograms to be used is three. In the present paper the statistical investigation, based on a Monte Carlo method, calls for hundreds of accelerograms, to be chosen within a sufficiently wide range of possible shapes.

The statistical analysis of vibratory responses is not made for design purposes, but it is intended to represent the "real" structural behaviour to which the ordinary design criteria, based on the design spectrum for an elastic analysis, have to be compared. To this purpose the parameters of the type shape of the accelerograms are made vary within proper ranges.

For the generation of the artificial motion, the programme SIMQKE from MIT–Dept. of Civil Eng. has been used (SIMQKE, 1976). The motion is given by

$$x(t) = I(t)\sum_{i=1}^{n} x_i \sin(\omega_i t + \varphi_i) \tag{1}$$

where the phase angles φ_i are random values and the amplitudes x_i are chosen so to match the given response spectrum all within its range of frequencies ω_i. $I(t)$ is the envelope curve which gives the amplitude time variation, with an initial starting branch, a steady middle branch corresponding to the stationary part and a final descending branch (see Fig. 2).

For the present application, a "compound" function for the envelope curve has been chosen with

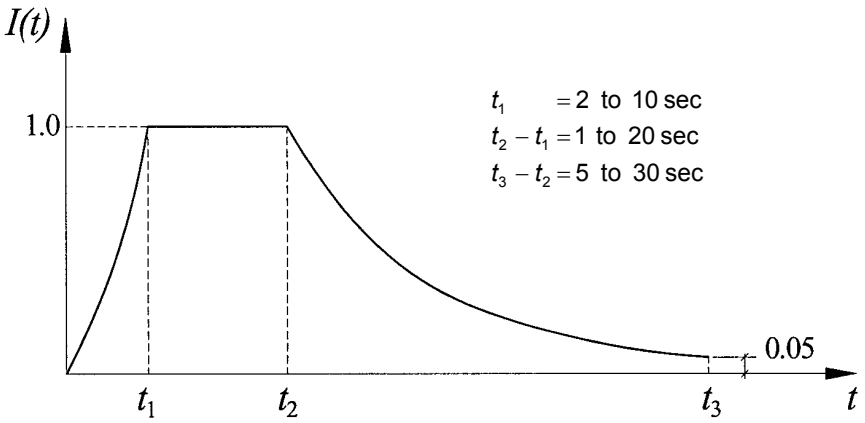

Figure 2. Envelope shape curve of ground motion.

$$
\begin{aligned}
I(t) &= (t/t_1)^2 \quad \text{for} \quad 0 \le t < t_1 \\
I(t) &= 1 \quad \text{for} \quad t_1 \le t \le t_2 \\
I(t) &= \mathrm{e}^{-\alpha(t-t_3)} \quad \text{for} \quad t_2 < t \le t_3
\end{aligned} \tag{2}
$$

The shape parameters have been generated as random variables according to an uniform distribution within the ranges

$$t_1 = 2 \text{ to } 10 \text{ sec} \qquad t_2 = 1 \text{ to } 20 \text{ sec} \qquad t_3 = 5 \text{ to } 30 \text{ sec} \tag{3}$$

Fig. 3 shows three of these accelerograms scaled to the peak ground acceleration PGA=1.0, joined by their response spectrum. The superposition of the spectra with the target one (EC8 response spectrum for subsoil class A) indicates the precision of the generation process.

The random variability of materials has been considered with the following assumptions. For the concrete, starting from a fixed characteristic value f_{ck}=40 MPa, the strength varies following a lognormal distribution defined by the mean $f_{cm}=f_{ck}+ks$ and by the standard deviation s=5 MPa, with k=1.551. For the reinforcing steel, starting from a fixed characteristic value f_{yk}=500 MPa, the yield stress varies following a lognormal distribution defined by the mean $f_{ym}=f_{yk}+ks$ and by the standard deviation s=30 MPa, with k=1.597. The geometrical parameters, related to the dimension of the structure, have been taken as deterministic with their nominal values.

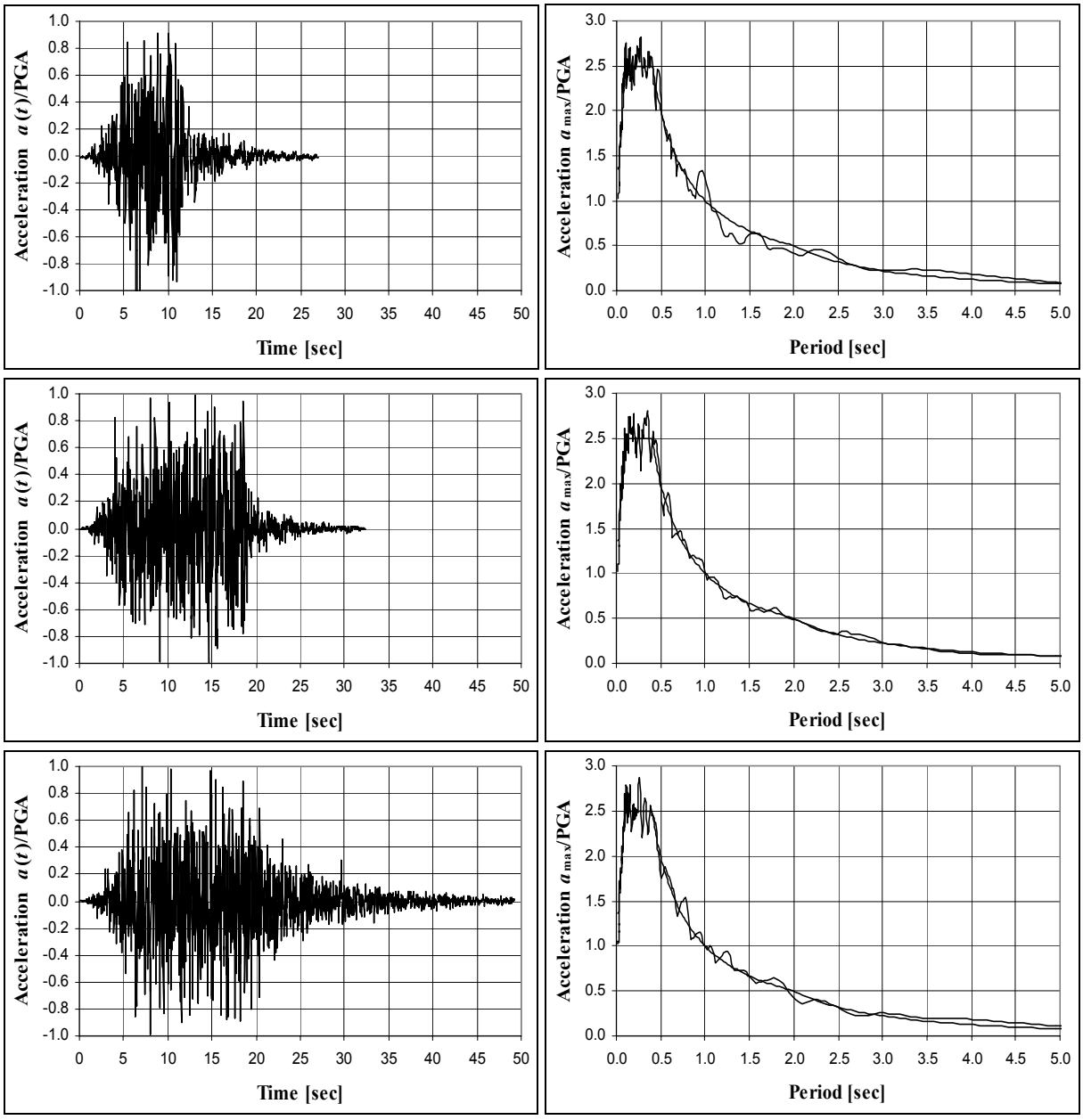

Figure 3. Sample of three artificial accelerograms and their response spectra.

3. STRUCTURAL ANALYSIS

The dynamic non-linear analysis for the one degree of freedom systems under examination is based on the ordinary motion equation

$$m\,\ddot{d}(t) + c\,\dot{d}(t) + k(d)d(t) = -m\,a(t) \tag{4}$$

where m is the vibrating mass, c is the viscous damping coefficient (assumed equal to 5% of the critical one), $k(d)$ is the degrading elastoplastic stiffness and $a(t)$ is the ground acceleration. The top displacement d of the structure is an unknown function of the time t. The static term, corresponding to the shear force $V(d)$ of the columns, is directly given as:

$$k(d)d(t) = V(d) = F(d) - \frac{N_{ad}}{h}d(t) \tag{5}$$

where the second term represents the second order effect of the vertical load N_{ad} acting on the columns and $F(d)$ is read on the proper force-displacement model as a function of the preceding load history.

The *F-d* function of the degrading elastoplastic stiffness has been derived from Takeda model (Takeda *et al.*, 1970), completed with a decreasing branch as introduced by Priestley *et al.* (1994) in order to represent the ultimate phase of failure. Fig. 4 shows the envelope curve of hysteretic cycles, where the limit points of the model correspond respectively to the first cracking of the critical section, to the yielding of reinforcement and to the compressive failure of concrete core (for more details see Biondini and Toniolo, 2000). In a previous work (Saisi and Toniolo, 1997) the algorithm has been verified versus pseudodynamic tests.

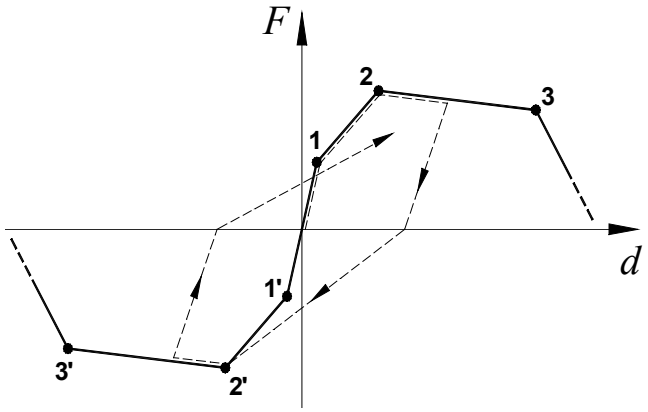

Figure 4. Degrading stiffness model.

The values of the limit points of the envelope curve of Fig. 4 for the two frames considered in the analysis are given in Table 1. The details of the frames and the calculation of the related structural parameters are given in Appendix. Note that for the calculation of the displacement d_3 at the end of the plastic phase, the length h_p of the plastic hinge had to be estimated. For this estimation the equation of Park and Paulay (1975) has been applied with the addition of the shift shear effect:

$$h_p \cong 0.08h_0 + 0.022\varnothing f_{sd} + d_{eff}/2 \quad [f_{sd} \text{ in MPa}] \tag{6}$$

with $\varnothing$ diameter of the longitudinal bars, f_{sd} design strength of the reinforcing steel, d_{eff} effective depth of the cross section and h_0 equal to the distance of the plastic hinge from the zero moment section.

The quoted model refers to a flexural mode of failure. This mode is ensured by the slenderness of the columns. In addition it is assumed that a proper capacity design ensures the full efficiency of the connections, so that the collapse of the overall structure comes from the failure of the critical sections of the columns. Their strength and ductility, as represented by the *F-d* model, give the seismic capacity of the structure.

Table 1. Co-ordinates of the model limit points: (a) monolithic frame; (b) hinged frame.

	F_1 [kN]	d_1 [mm]	F_2 [kN]	d_2 [mm]	F_3 [kN]	d_3 [mm]
(a)	8.235	4.8	34.392	120.8	28.160	704.6
(b)	8.137	5.0	33.225	144.7	28.567	1035.5

For the integration of the motion equation the ordinary Newmark step by step numerical method (Newmark, 1959) has been applied, with β=0.25 and γ=0.50 (mean acceleration method). A tangent approximation of the degrading stiffness ensures, together with the displacement control process, the good convergence of the numerical algorithm.

Fig. 5 gives the vibration curves computed for the three accelerograms of Fig. 3, both for the cast-in-situ frame with rigid joint connections and for the precast frame with hinged joint connections. Any set of vibration curves is computed with increasing values of $\alpha_g = a_g/g$ (a_g is the peak groung acceleration - PGA), starting from α_g=0.30 with increments $\Delta\alpha_g$=0.05 (in the figure only some of these curves are drawn). The collapse is pointed out by the loss of the vibratory equilibrium, with unlimited amplification of the displacement, due to the fast increase of the second order effects on the falling stiffness of the structure. For the three cases here considered the collapse occurred at the intensities $\alpha_{g\max}$ listed in Tab. 2.

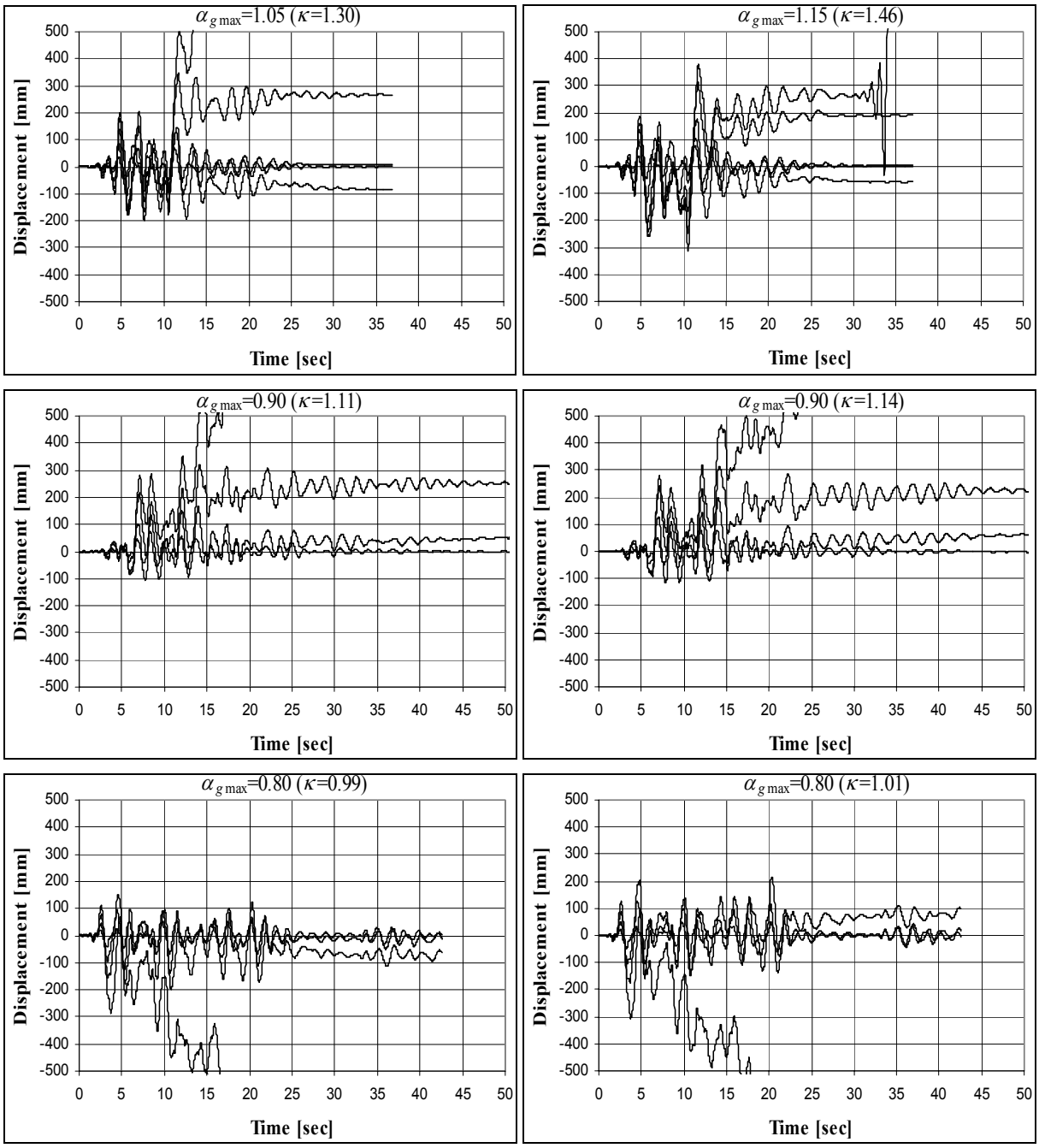

(a) (b)

Figure 5. Vibration curves for the accelerograms given in Fig. 2 for PGA values in the range α_g=0.30, 0.50, 0.70, …, $\alpha_{g\max}$: (a) monolithic arrangement; (b) hinged arrangement.

Table 2. Collapse intensities $\alpha_{g\max}$ for the three accelrograms in Fig. 3.

$\alpha_{g\max}$	Monolithic Frame	Hinged Frame
(1)	1.05	1.15
(2)	0.90	0.90
(3)	0.80	0.80

These computations have been repeated 1000 times with seismic actions chosen in the random way specified in chapter 2. The computed responses are represented by the overstrength ratio κ between the ultimate capacity $\alpha_{g\max}$ of the structure and the design strength $\overline{\alpha}_g$:

$$\kappa = \frac{\alpha_{g\max}}{\overline{\alpha}_g} \tag{7}$$

The design ultimate strength $\overline{\alpha}_g$ is derived from EC8 rules as follows:

$$\overline{\alpha}_g = \frac{q}{2.5\eta(T)}\frac{F_d}{W} \tag{8}$$

where the behaviour factor is taken $q = 5$, $\eta(T)$ represents the decresing function of the elastic response spectrum evaluated at the natural vibration period T, W is the weight of the vibrating deck and F_d is the ultimate limit value of the seismic force expressed in terms of the resistant moments M_{rd} of the critical sections (see Table A.1 of Appendix):

$$\begin{aligned} F_d &= 2M_{rd}/h \quad \text{for the cast - in - situ frame} \\ F_d &= M_{rd}/h \quad \text{for the precast frame} \end{aligned} \tag{9}$$

For a subsoil class A EC8 gives $(T_C = 0.4\,\text{sec},\ T_D = 2.0\,\text{sec})$:

$$\begin{aligned} \eta(T) &= \frac{T_C}{T} \geq \frac{0.20}{2.5}q \quad \text{for } T_C \leq T \leq T_D \\ \eta(T) &= \frac{T_C T_D}{T^2} \geq \frac{0.20}{2.5}q \quad \text{for } T_D < T \end{aligned} \tag{10}$$

so that the design ultimate seismic strengths are:

$$\begin{aligned} \overline{\alpha}_g &= 0.81 \quad \text{for the cast - in - situ frame} \\ \overline{\alpha}_g &= 0.79 \quad \text{for the precast frame} \end{aligned} \tag{11}$$

The overstrength κ is the basic measure of the reliability of the design rules of the Eurocode 8, since it represents the direct comparison between the "actual" experimented strength and the "design" computed strength of the structure. In probabilistic terms, its characteristic lower value should be 1 for a good reliability.

4. RESULTS OF THE ANALYSIS AND CONCLUDING REMARKS

The results of the analyses are summarised in the regression diagram of Fig. 6, which shows the correlation between the responses of the two structures for the sample set of 1000 accelerograms. The diagram refers to the overstrength ratio κ, computed with reference to the ultimate design strength $\overline{\alpha}_g$ (correlation factor $\rho_\kappa = 0.884$), for the cast-in-situ frame in abscissa and for the precast frame in ordinate. Such diagram allow a direct comparison between the seismic behaviour of both the cast-in-situ and the precast frame, showing the substantial equivalence of any couple of values, with small differences.

In statistical terms, a more meaningful comparison of the responses can be deduced from the density distributions of the overstrength ratio κ. Such distributions are shown in Fig. 7, together with their fitting curves drawn according to the lognormal model. Based on such model, the characteristic 5% fractile and the mean values listed in Tab. 3 are deduced. The characteristic values for the overstrength ratio are somewhat higher than $\kappa = 1$, which is the limit of full reliability of the analysis. The margin can compensate the approximations of the analytical model.

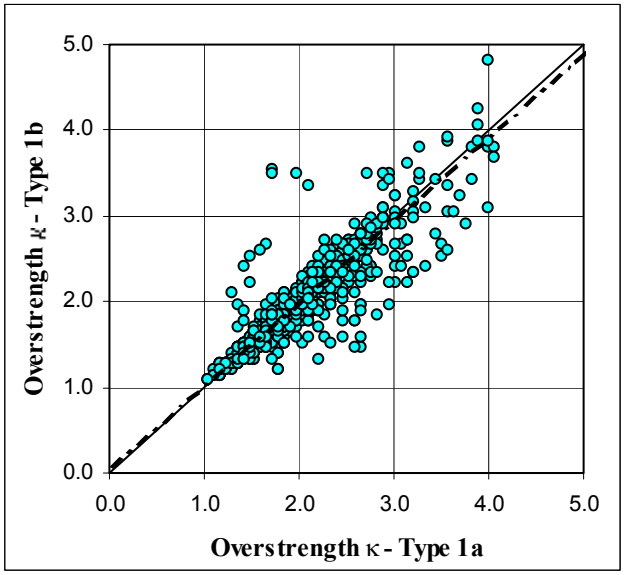

Figure 6. Correlation diagram of the overstrength ratio κ for both the monolithic and the hinged frames (1000 simulations).

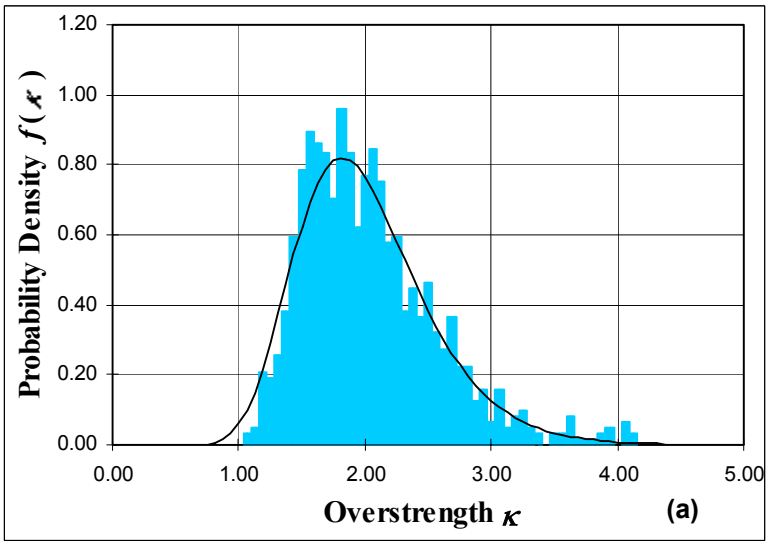

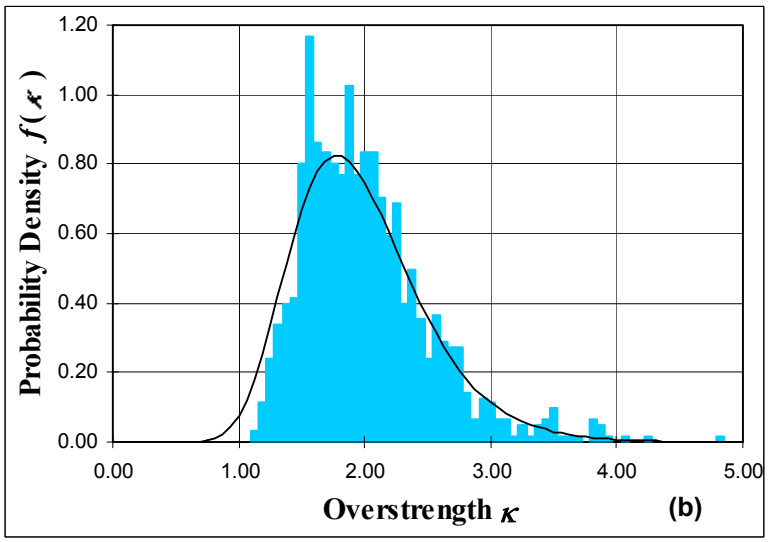

Figure 7. Distribution diagrams of the overstrength κ for both (a) the monolithic and (b) the hinged frames.

Table 3. Mean and characteristic (fractile 5%) values of the overstrength κ (lognormal model).

	Monolithic Frame	Hinged Frame
Mean κ_m	2.01	1.91
Characteristic $\kappa_{0.05}$	1.27	1.27

The results show first a very good correspondence between the design estimate deduced from EC8 rules and the "real" ultimate capacity computed from the analysis. This confirms also the reliability of the behaviour factor q = 5 assumed in the present comparative calibration. The results clearly show also that the precast frame with hinged beams, having critical sections located at the base of the columns and dimensioned for the corresponding clamping moments, is able to dissipate the same quantity of energy which the monolithic frame dissipates in its more numerous critical sections, being dimensioned for halved moments. Naturally these conclusions refer only to the particular type of structure represented by the couple of test frames examined in the analysis and cannot be extended in general.

Some additional considerations must be added with reference to the representativeness of the artificial accelerograms assumed to simulate earthquake action. Actual recorded accelerograms, contrary to the artificial ones, are in general poor of frequencies and may lead, for the same value of the peak ground acceleration, to much different responses of the structure. They have a rough compatibility with the response spectra of the code and are of insufficient numerousness for the computation of stabilised statistical values. These characteristics introduce additional uncertainties in the comparison with their design model and would lead to a very large scattering of the responses as shown by Biondini, Toniolo and Tsionis (2001). This indicates the necessity to cover the uncertainties of the design model of seismic action with an additional safety margin (or a decrease of the q-factor from 5 to 4.5).

Finally the value of the behaviour factor deduced for the one storey frames dealt with in the present work doesn't include the possible additional resources due to structural redundancy represented by the ratio "α_u/α_1" of EC8. In fact the two test structures considered in the analysis are statically determinate systems with one degree of freedom. The real buildings with many columns and high degree of support redundancy may have sensible higher seismic capacity due to the possible redistribution of actions on the different elements of the structure.

ACKNOWLEDGEMENTS

The present research has been supported by "Cofinanziamento MURST–COFIN99".

REFERENCES

Biondini F. and Toniolo G., Comparative Analysis of the Seismic Response of Precast and Cast-in-situ Frames. *Studies and Researches*, Graduate School for Concrete Structures, **21**, 1-17, 2000.

Biondini F., Toniolo G. and G. Tsionis, Design Reliability of Cast-in-situ and Precast Frames under Recorded Earthquakes. *Studies and Researches*, Graduate School for Concrete Structures, Politecnico di Milano, **22**, 2001.

Biondini F. and Toniolo G., Probabilistic Calibration of Behaviour of EC8 for cast-in-situ- and Precast frames, *Proceedings of 17th BIBM Congress*, Instanbul, 2002.

CEB, *Reinforced Concrete Elements Under Cyclic Loading. State-of-the-Art Report*. Bulletin **230**,1996.

CEB, *RC Frames Under Earthquake Loading. State-of-the-Art Report*. Bulletin **231**,1996.

CEN [2001] *prEN 1998-1 (Draft May 2001). Eurocode 8: Design of Structures for Earthquake Resistance. General Rules, Seismic Actions and Rules for Buildings* , European Committee for Standardization, Brussels, 2001.

Clough R.W. and Johnston S.B., Effect of Stiffness Degradation on Earthquake Ductility Requirements, *Proc. Japan Earthquake Eng. Symposium*, Tokyo, Japan, 227-232, 1966.

Fardis M.N., Member-Type Models for the Nonlinear Seismic Response Analysis of Reinforced Concrete Structures, *Experimental and Numerical Methods in Earthquake Engineering*, Donea J., Jones P.M. (Eds.), Kluwer, Dordrecht, 247-280, 1991.

Fardis M.N. Seismic Design and Response of Bare and Masonry-Infilled Reinforced Concrete Buildings. Part I: Bare Structures, *Journal of Earthquake Engineering*, **1**(1), 219-256, 1997.

Gibertson M., The Response of Nonlinear Multi-Storey Structures Subjected to Earthquake Excitations, *Earthquake Engineering Research laboratory*, Pasadena (CA), 1967.

Kunnath S.K., Reinhorn A.M. and Park Y.J. Analytical Modeling of Inelastic Seismic Response of R/C Structures, *ASCE Journal of Structural Engineering*, **116**(4), 996-1017, 1990.
Newmark, N.M.. A Method of Computation for Structural Dynamics. *ASCE Journal of the Engineering Mechanics Division*, **85**(3), 67-94, 1959.
Park R. and Pauley T. *Reinforced Concrete Structures*. John Wiley & Sons, 1975.
Pauley T. and Priestley M.J.N. *Seismic Design of Reinforced Concrete and Masonry Buildings*. John Wiley & Sons, 1992.
Priestley M.J.N., Verma R. and Xiao Y., Seismic Shear Strength of R.C. Columns, *ASCE Journal of Structural Engineering*, **120**(8), 2310-2329, 1994.
Qi X. and Pantazopoulou S.J., Response of RC Frame under Lateral Loads, *ASCE Journal of Structural Engineering*, **117**, 1167-1188, 1991.
Saatcioglu M. and Ozcebe G., Response of Reinforced Concrete Columns to Simulated Seismic Loading, *ACI Journal*, **1**, 3-12, 1989.
Saisi A. and Toniolo G., Experimental and Numerical Analysis of the Seismic Behaviour of the R.C. Columns of Precast Buildings, *Proceedings of Giornate AICAP*, 1997 (in Italian).
SIMQKE, *A Program for Artificial Ground Motion Generation. User's Manual and Documentation*, NISEE Computer Applications, Department of Civil Engineering, Massachusetts Institute of Technology, 1976.
Takeda T., Sozen M.A. and Nielsen N.N. Reinforced Concrete Response to Simulated Earthquakes, *ASCE Journal of the Structural Division*, **96**(12), 2557-2573, 1970.
Toniolo G., The Seismic Design of Precast Concrete Structures in the New Eurocode 8, *Proceedings of 17th BIBM Congress*, Instanbul, 2002.

APPENDIX: DESIGN DATA OF THE FRAMES

The frame in the two arrangements described in Fig. A.1 is considered. A total load on the roof leading to an axial force on the columns N_{ad}=216.0 kN and to a seismic weight $2W = 2 \times 187.2\,\text{kN}$ is assumed. The dimensions come from the serviceability requirements and from the non seismic conditions. With the reinforcement indicated in the sections of Fig. A.2 and with the following material properties:

$$\begin{aligned} f_{cd} &= f_{ck}/\gamma_c = 40/1.5 = 26.7\,\text{N/mm}^2 \quad (E_c = 28\,\text{kN/mm}^2, \varepsilon_{cu} = 3.5‰) \\ f_{sd} &= f_{yk}/\gamma_s = 500/1.15 = 437\,\text{N/mm}^2 \quad (E_s = 206\ \text{kN/mm}^2, \varepsilon_y = 2.4‰) \end{aligned} \tag{A.1}$$

the following resistant moments are obtained:

$$\begin{aligned} M_{rd} &= M_{rd}(N_{ad}) = 91.07\,\text{kNm} \quad \text{for the cast - in - situ frame} \\ M_{rd} &= M_{rd}(N_{ad}) = 177.56\,\text{kNm} \quad \text{for the precast frame} \end{aligned} \tag{A.2}$$

The reinforcement of middle-span section of the beam has been proportioned with a non-seismic design on the base of the corresponding bending moment. At the end of the beam the resistant moment remains larger than at the connected column.

In Tab. A.1, together with the computed resistant moments, the values of the following parameters are summarised:

- the resistant moments M_{rd} computed above;
- the specific value of the axial load $\nu_E = N_{ad}/N_E$, being $N_E \cong 10k_\varphi/h^2$;
- the flexural stiffness k_φ of the sections, computed as $k_\varphi = M_y/\chi_y$ where the moment M_y is assumed equal to ¾ of the corresponding resistant moment and where the curvature χ_y is deduced on the cracked elastic section with the eccentricity $e = M_y/N_{ad}$;
- the traslatory stiffness k_δ of the columns, computed as $k_\delta = 12k_\varphi/h^3 - N_{ad}/h$ for the monolithic arrangement and $k_\delta = 3k_\varphi/h^3 - N_{ad}/h$ for the hinged arrangement, where the term proportional to the axial load represents the second order effect;
- the self vibration period $T = 2\pi\sqrt{m/k_\delta}$ ($m = W/g$, where g is the gravity constant);
- the yield displacement d_y, computed as $d_y = \chi_y h^2/6$ for the monolithic arrangement and $d_y = \chi_y h^2/3$ for the hinged arrangement.

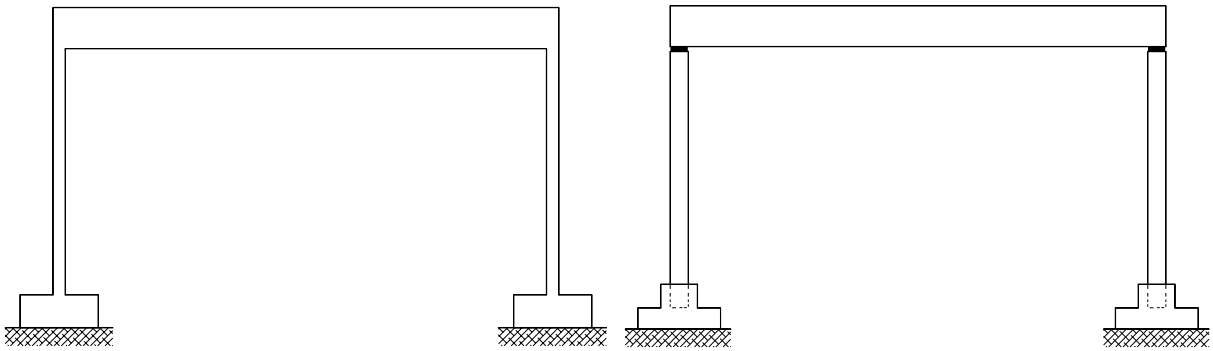

Figure A.1. Type frame: (a) monolithic arrangement; (b) hinged arrangement.

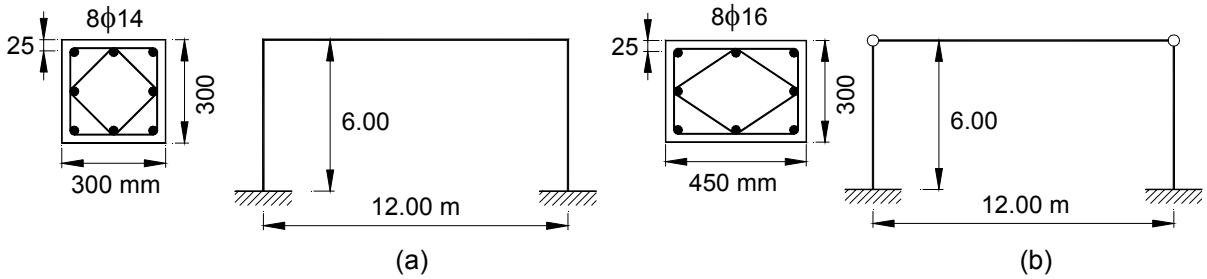

Figure A.2. Scheme of the frames and details of the reinforcement: (a) monolithic arrangement; (b) hinged arrangement.

Table A.1. Design data of prototypes: (a) monolithic frame; (b) hinged frame.

	M_{rd} [kNm]	ν_E	k_φ [kNm^2]	k_δ [kN/m]	T [sec]	d_y [mm]
(a)	91.07	0.152	5122.7	248.6	1.87	106.7
(b)	177.56	0.047	16535.3	193.7	2.12	128.9